

AN ABSTRACT OF THE THESIS OF

Nichole I. Victory for the degree of Master of Science in Civil Engineering
presented on June 13, 2007.

Title: Quantification of Advection and Dispersion in Lateral Subsurface Flowpaths
at the Hillslope-scale

Abstract approved:

Jonathan D. Istok

It is becoming increasingly important to understand fundamental hillslope-scale hydrological processes. Most hillslope-scale transport experiments have generally focused on conceptual findings or other aspect of flow behavior, rather than the quantification of the mass transport mechanisms of advection and dispersion. When the velocities have been quantified, dispersion has been mentioned as present, but has not yet quantified. This study uses a natural gradient well-injection tracer test to characterize solute transport in lateral subsurface flowpaths. The breakthrough curves obtained from the tracer tests were analyzed using traditional hillslope hydrology methods for calculating velocities, time to peak and the Mosley [1982] method, as well as CXTFIT, a program that computes average velocity and dispersion coefficients for breakthrough curves by fitting experimental data to the 1-Dimensional convective-dispersion equation using a non-linear least-squares regression technique.

Well injection tracer tests at the WS10 hillslope showed advection and dispersion rates larger than reported from laboratory studies and comparable rates to those reported from field studies. Lateral preferential flowpaths appeared to significantly reduce travel time through the study hillslope. However, once tracer was stored in the subsurface, the travel times and average velocities depended

largely on the applied driving force (i.e. intensity and duration of precipitation and/or injection). The tracer tests also illustrated that as less tracer remained in the flowpath the amount of water required to remove a quantity of mass increased.

Through the quantification of advection and dispersion in Experiment 1, it was shown not only that one flowpath had a larger advective velocity but also mixed with the tracer-free water more due to its higher velocity. In addition, the dispersion coefficients showed that while Inj1 and Inj2 have very similar BTCs, Inj2's dispersion coefficient was about twice that of Inj1's, indicating that Inj2 spread longitudinally more than Inj1. Through the quantification of advection and dispersion in Experiment 2, the large effect of stored water on apparent dispersion was illustrated. As stored water plays a leading role in the hillslope hydrology, accounting for the dispersion that results from storage is imperative to accurately describing internal hillslope hydrological processes.

© Copyright by Nichole I. Victory
June 13, 2007
All Rights Reserved

Quantification of Advection and Dispersion in Lateral Subsurface Flowpaths at the
Hillslope-scale

by
Nichole I. Victory

A THESIS

submitted to

Oregon State University

in partial fulfillment of
the requirements for the
degree of

Master of Science

Presented June 13, 2007
Commencement June 2008

Master of Science thesis of Nichole I. Victory presented on June 13, 2007.

APPROVED:

Major Professor, representing Civil Engineering

Head of the Department of Civil, Construction and Environmental Engineering

Dean of the Graduate School

I understand that my thesis will become part of the permanent collection of Oregon State University libraries. My signature below authorizes release of my thesis to any reader upon request.

Nichole I. Victory, Author

ACKNOWLEDGEMENTS

I wish to express my sincere thanks to the following people for their assistance. Without their support this work would not have been possible.

Lukas Potts
Jesse Jones
Willem van Verseveld
Chris Graham
John Moreau
Kathy Keable
Jeff McDonnell
Jack Istok

And most of all, my family! My husband, Joe Dunn; my parents, Lynn and Clarence Victory; and my brother, Mark Victory.

TABLE OF CONTENTS

	<u>Page</u>
1. INTRODUCTION	1
2. SITE DESCRIPTION	5
3. METHODS	7
3.1. Site and Experimental Set-up	7
3.1.1. WS10 Well installations	7
3.2. Two Tracer Experiments	10
3.2.1. Experiment One	11
3.2.2. Experiment Two	12
4.1. Experiment One.....	14
4.1.1. Inj1 in well E1	14
4.1.2. Inj2 in well C2	17
4.1.3. Flushes	19
4.2. Experiment Two.....	22
5. DISCUSSION: CHARACTERIZATION OF LATERAL SUBSURFACE FLOW.....	25
5.1. Advection and dispersion quantified in two flowpaths at the hillslope- scale: Experiment 1	25
5.2. Advection and dispersion quantified in one flowpath under different flow conditions: Experiment 2	29
5.3. Comparison of velocities and dispersivities with other studies.....	32
5.4. Why quantify velocities and dispersivities?.....	35
6. CONCLUSIONS	37
 BIBLIOGRAPHY	 38
 APPENDICES	 41
Appendix A: Dynamic Cone Penetrometer Profile	42
Appendix B: Volume Equivalent Precipitation calculation	43
Appendix C: Determination of Mass recovered per well.....	44
Appendix D: Theoretical concentration drop due to flowpath drop	45

TABLE OF FIGURES

<u>Figure</u>	<u>Page</u>
1: Study Site with trench, well locations and seep location indicated.....	6
2: Well profile, (values in meters)	8
3: BTC for Inj1 with evidence of additional concentration rise due to precipitation 2 days post-injection.....	15
4: Inj1 calibration of in-situ field ISE (installed in the stilling basin) to the IC in the laboratory	17
5: BTC Inj2 with evidence of additional concentration rise due to a tracer-free water flush 2 days post-injection.....	18
6: Inj2 calibration of in-situ field ISE (installed in the stilling basin) to the IC in the laboratory	19
7: Cumulative mass recovered and cumulative water added (throughout the flushes) as a function of time from beginning of Inj1	20
8: CXTFIT results for calculated velocity and dispersion coefficient for the E1 flushes.....	21
9: CXTFIT results for calculated velocity and dispersion coefficient for the C2 flushes.....	21
10: BTC for Inj3 showing injection and flush periods as well as the drops in volumetric flowrate and mass ratios during injection interruptions.....	23
11: Theoretical drop in concentration due to decrease flowpath volumetric flowrate and dilution from seep flow	24
12: CXTFIT results for calculates of velocity and dispersion coefficient based on relative mass out of the trench during injection and flush phases of Inj3	24
13: Initial BTCs Inj1 and Inj2	28

TABLE OF TABLES

<u>Table</u>	<u>Page</u>
1: Injection Summary.....	11
2: Injection parameters and breakthrough curve results	16
3: Summary of Velocities, Dispersion Coefficients and Dispersivities for Inj1, Inj2 and Inj3	16
4: Assumptions by method (X indicates assumption satisfied).....	30
5: Velocities calculated from Experiments 1 and 2, Harr and McGuire for WS10 hillslope	32
6: Empirical Values for unconsolidated porous media [Schnoor, 1996]	35
7: CXTFIT calculated values from Experiments 1 and 2	35

LIST OF APPENDIX FIGURES

<u>Figure</u>	<u>Page</u>
1: Dynamic Cone Penetrometer profile at well C2.....	42
2: Dynamic Cone Penetrometer profile at well E1	42
3: Flowchart of hillslope system with well injection	46

Quantification of Advection and Dispersion in Lateral Subsurface Flowpaths at the Hillslope-scale

1. Introduction

Numerous studies have examined water transport through porous media in the laboratory under controlled conditions [Brusseu, 1993; Hutchison et al, 2003; Maraqa et al, 1997; Vanderborght, 2000, 2002] and in the field, under less controlled conditions [Hewlett and Hibbert, 1963; Harr, 1977; Tsuboyama et al, 1994; Rodhe et al, 1996; Anderson et al, 1997; Nyberg et al, 1999]. Laboratory-scale experiments have quantified how parameters vary with flow conditions (i.e. unsaturated vs. saturated [Maraqa et al, 1997; Hutchison et al, 2003]), and material properties (i.e., consolidated vs. non-consolidated). The quantitative transport descriptions from such laboratory experiments have resulted from the ability to create boundaries and homogeneous hydraulic properties, accurately control boundary conditions and flowrates, isolate the system from outside influences (i.e. precipitation, upslope drainage, etc.), and fully characterize the porous media. Most importantly, the ability to manipulate one variable or parameter while keeping all others constant has been an invaluable tool in the laboratory for investigating transport mechanisms. In the field, attempts to create boundaries and control boundary conditions have included the use of barriers [Anderson, 1997; Brooks, 2004], cut-trenches [Mosley, 1982; Tsuboyama et al, 1994], covered fields [Nyberg et al, 1999; Rodhe et al, 1996], and artificial irrigation [Anderson et al, 1997; Tsuboyama et al, 1994]. Obviously, laboratory-like control is not possible in the field. Hillslope-scale experiments aimed at observing subsurface flow behavior have relied passively on natural precipitation events [Harr, 1977; McGuire et al, 2007], the use of irrigators or sprinklers to create "controlled" precipitation events [Tsuboyama et al, 1994; Anderson et al,

1997; Nyberg et al, 1999], and the tagging of water with tracers [Tsuboyama et al, 1994; Anderson et al, 1997; McGuire et al, 2007].

While assessing a larger and therefore likely more representative area than found in a laboratory, hillslope-scale experiments illustrate the degree of variability inherent in the natural environment [Beven, 2006]. To date, mainly qualitative descriptions of observed breakthrough curves (BTCs) and subsurface flow path transport characteristics have been made at the hillslope-scale. This is due to the difficulty in isolating a hillslope control volume in the field – necessary for quantifying hillslope-scale flow and transport. Comparisons of laboratory and field study results have revealed differences due to field-scale heterogeneity [Gelhar, 1992].

To better characterize the internal hydrologic processes and the effects of scale, more field experiments are needed [Sidle, 2006]. These experiments not only need to bridge the gap between laboratory and field scale observations [Gelhar, 1992], but also to bridge the gap between field observations and model predictions [Beven, 2006]. Advection and dispersion, the major mechanisms in mass transport processes [Schnoor, 1996], are important parameters to quantify when observing the flow and transport of water through the subsurface. Many field-based lateral subsurface flow studies at the hillslope-scale have reported observed velocities, but have generally focused on conceptual findings or other qualitative aspects of the flow behavior [Anderson et al, 1997; Nyberg et al, 1999; McGuire et al, 2007]. In addition, reported advective velocities include time to peak [McGuire et al, 2007; Anderson et al, 1997], time to center of mass (CoM) [Mosley, 1982], average, and Darcy [Harr, 1977] velocities. Often it is not clear which velocity is reported as they are merely reported as “subsurface flow

velocities" [McGuire et al, 2007]. While some hillslope studies have "observed" dispersion [Tsuboyama et al, 1994; Anderson et al, 1997; McGuire et al, 2007], or the ramifications resulting from a lack of accounting for dispersion [Jones et al, 2006], no field-based hillslope-scale studies have calculated the amount of dispersion from the BTCs observed.

The advection-dispersion equation (ADE) is used to describe solute transport and accounts for the advective and dispersive components. The hydrodynamic dispersion coefficient quantifies the amount of hydrodynamic dispersion or the amount a solute spreads and is diluted in addition to its advective movement [Bedient et al, 1997]. By fitting the ADE to an experimental BTC, using a non-linear least-squares regression technique, the average velocity (advective) and the hydrodynamic dispersion coefficient may be solved for simultaneously.

Dispersivity is a scaling value that relates a flowpaths average velocity to its dispersion coefficient and is thought to be a characteristic of soil [Domenico & Schwartz, 1998] as well as the scale observed [Schnoor, 1996; Gelhar, 1992]. The relationship between the dispersion coefficient and average velocity is linear [Domenico & Schwartz, 1998] and dispersivities are calculated using the equation:

$$\alpha = \frac{D}{v} \quad (2)$$

where α is the dispersivity [m], D is the hydrodynamic dispersion coefficient [m^2/hr], and v is the average (average pore-water) velocity [m/hr]. Dispersivity is a constant based on location and is more easily used for comparison purposes than D , which is dependent on the average velocity.

This study uses a natural gradient well-injection technique, used in groundwater studies, to characterize and improve the understanding of lateral subsurface flowpaths on a well-studied hillslope in the HJ Andrews (HJA) Experimental Forest, Western Oregon, USA. The specific objectives of this study are to quantify advective velocities and dispersion coefficients at the hillslope-scale and to use the determined values to: 1) compare transport in two distinct flowpaths; 2) compare transport in one flowpath under different injection conditions; 3) compare to previous studies; and 4) discuss how these measurements may add to the conceptualization of internal hillslope hydrological processes.

2. Site Description

The HJA is located in the Willamette National Forest in the Oregon Cascade Mountain Range. This study focused on a south-facing hillslope in a 10.2 ha watershed known as Watershed 10 (WS10). The WS10 hillslope was extensively studied by Harr [1977], and more recently by McGuire [2007]. The mean annual precipitation at the site is 2350 mm, which falls mainly between October and April, during low intensity, long-duration frontal storms [Harr, 1977]. While the streamflow is perennial, flows are considerably higher during the winter wet-season than the low base flow in the summer dry-season. Clear-cut in 1975, WS10 is dominated by second growth Douglas-fir [Jones, 2000]. The elevation ranges from 425 to 700 m. Due to the steep terrain ($\sim 48^\circ$ near the stream), the soils are shallow [Rothacher et al, 1967], ranging from 0.5 m at the lower elevations to 5 m at the ridgeline [van Verseveld, unpublished data]. Ranken [1974] analyzed 452 soil cores from 11 soil pits in WS10 and reported the mean soil K_s (from Pit 3) decreased from 8.9 m/hr at 30 cm to 0.05 m/hr at 160 cm, and often changed abruptly within the profile [Ranken, 1974]. Soil porosity varied between 60-70% at the surface, and decreased to $\sim 50\%$ at depth [Ranken, 1974]. Surface soils in WS10 are highly permeable, while sub-surface soils are less permeable. The subsurface consists of saprolite underlain by rock from pyroclastic flows [Ranken, 1974].

McGuire installed a trench at the base of the WS10 hillslope in 2000. The 10-meter long trench cemented to the bedrock streambed captures and channels water from the 48° hillslope into a stilling basin (Figure 1) to measure discharge from the hillslope. Previous debris-flows scoured the channel leaving the base of the hillslope devoid of a riparian zone [Harr, 1977]. This allows analysis of the

hillslope outflow without the influence of the riparian zone. At the upslope end of the trench a seep continuously supplies water to the trench. The trench collects lateral subsurface flow from the hillslope, except for the flow that may bypass the trench (on either side) or deeply percolate into the bedrock. This seep may be related to the presence of a north-northwesterly antidesitic, vertical dike that manifests itself as a localized zone of saturated soil [Swanson and James, 1975; Harr, 1977].

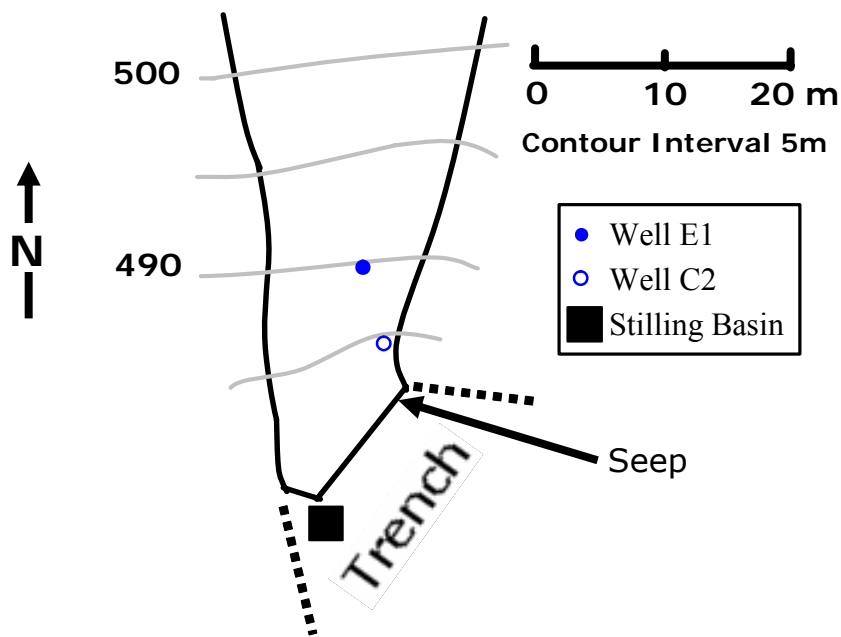


Figure 1: Study Site with trench, well locations and seep location indicated

3. Methods

3.1. *Site and Experimental Set-up*

3.1.1. *WS10 Well installations*

A grid-like pattern of wells has been installed on the WS10 hillslope [van Verseveld, unpublished data]. A hand-auger bored holes for the well installations. Constructed of 3.8 cm O.D., 3.2 cm I.D. PVC pipe each of the wells are perforated and screened over the bottom 20 cm. Dynamic cone penetrometer, Easting-Northing, and elevation data [van Verseveld, unpublished data] are available for each of the wells on the hill in WS10, as well as for the trench.

Two wells, C2 and E1 were used for the experiments (Figure 1). Well E1 is located approximately 15 m upslope from the middle of the trench. The soil depth at E1 is 1.23 m, while the well penetrates the top 0.81 m of soil (Figure 2). Dynamic cone penetrometer data shows the resistance from the soil surface to the well base is relatively constant and low (<20 knocks per 10 cm, Appendix A). Below the E1 well base, the resistance increases sharply at two depths with a region in between that has a relatively constant and low resistance, (97 and 120 m are where the resistance increases). At 0.81 m, the average total porosity is approximately 0.62 and the soil K_s is approximately 6.6 m/hr [Ranken, 1974]. Well C2 is located approximately 9 m upslope from the middle of the trench. The soil depth at C2 is 0.43 m, while C2 penetrates the top 0.35 m of soil, Figure 2. The dynamic cone penetrometer data gathered at C2 illustrate that the resistance from the soil surface to the well base is fairly constant and relatively low (<20 knocks per 10 cm), Appendix A). Below the C2 well base, the resistance increases dramatically (over the next 40 cm) to the bedrock. At 0.35 m, the

average porosity is approximately 0.67, and the soil K_s is approximately 8.9 m/hr [Ranken, 1974].

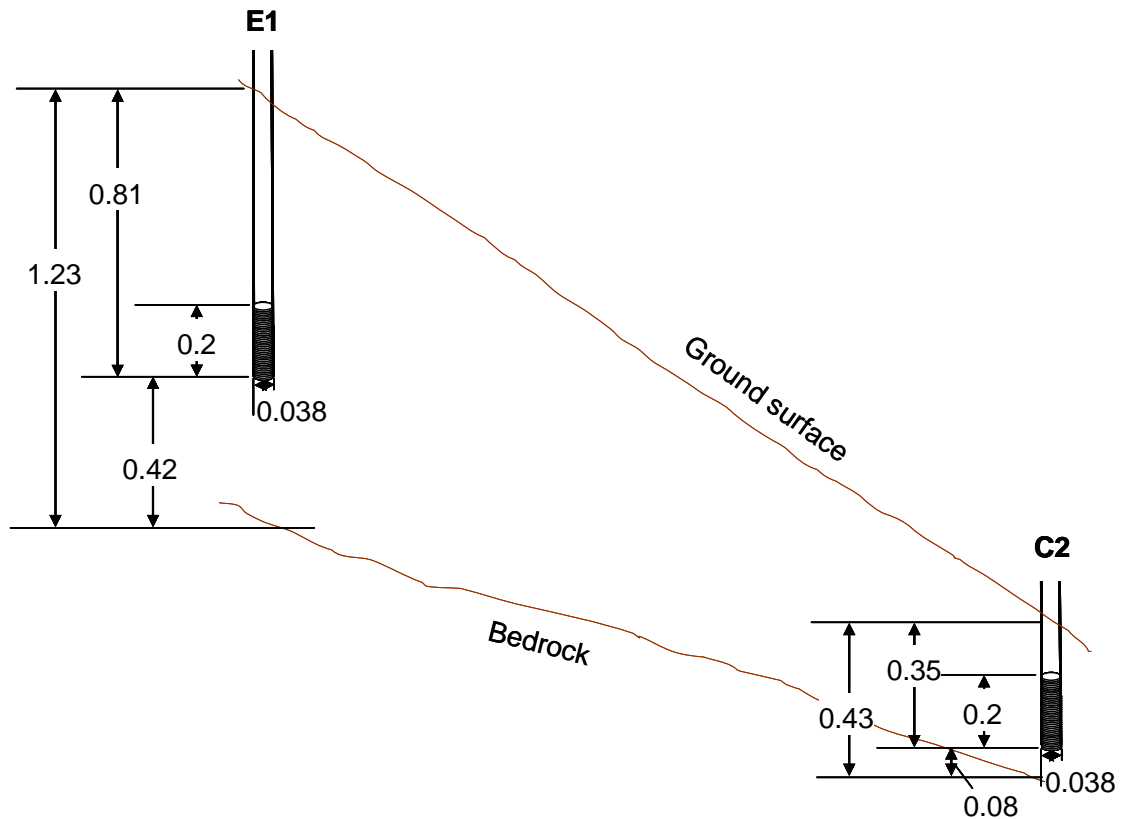


Figure 2: Well profile, (values in meters)

3.1.2. Experimental Set-up

Tracer injections were performed in Wells E1 and C2. A Masterflex® precision peristaltic pump (Cole Parmer Model# 7518-00) controlled the injection volumetric flowrate (Q_{inj}). Q_{inj} was measured volumetrically by recording the time required to pump 1L from the carboy, or by collecting a known volume of the outflow from the injection line into a graduated cylinder. Injection solution was pumped from a carboy into each well. Stream water was used for the tracer-free

water injections, while lithium bromide solutions were used for the tracer injections.

Water collected in the trench is piped into a stilling basin where the residence time varied between 0.13 and 12 minutes over the course of the experiments, depending on the seep flow. Two capacitance rods (TruTrack, Model# WT-VO 500) measured water height and were used to calibrate the water level in the basin to the volumetric flow rate of water through the v-notch weir. A bromide ion-selective electrode (ISE) (Instrumentation Northwest) measured the subsurface stormflow trench bromide concentration, $[\text{Br}^-]_{\text{trench}}$, as well as the air and water temperatures in the stilling basin. Data was recorded using a CR10 datalogger (Campbell Scientific). To verify the accuracy of the ISE measurements, grab samples were taken from the trench outflow during each of the injections. Grab samples were also obtained from the seep during the injections. All of the grab samples were analyzed in the laboratory using a D-120 Ion Chromatograph (IC) (Dionex, Sunnyvale, CA).

3.1.3. Calculations

Three methods were used to calculate subsurface lateral flow velocities: the time to peak; time to center of mass (CoM) [Mosley, 1982]; and the CXTFIT method [Toride, 1999]. The time to peak and the time to CoM methods, both define the travel distance as the linear distance between the injection point and the measurement point. The time to peak method defines the travel time as the time to the peak of the BTC from the beginning of the injection. In the time to CoM method, the mean travel time is defined as the time to the center of mass of the BTC from the center of mass of the injection [Mosley, 1982]. CXTFIT 2.1 is a one-dimensional analytical model that uses a non-linear least-squares regression with

the ADE to fit transport parameters (velocities and dispersion coefficients) to tracer data [Toride, 1999]. The cumulative mass recovered was used in relation to the total mass recovered in order to analyze the behavior of the tracer recovered, not the tracer that became stored in the subsurface. To do this we used the ratio:

$$\frac{\text{cumulative mass recovered at time } t}{\text{total mass recovered}}$$

where t refers to the time from the beginning of tracer injection to normalize the concentration data for input into CXTFIT. Solutions fitted to experimental results based on the ADE allow parameters (e.g. average pore-water velocity and dispersion coefficient) to be quantified [Toride et al, 1999].

3.2. Two Tracer Experiments

Two tracer experiments were conducted between April 12 and June 20, 2006. The first experiment, Experiment 1, consisted of a one hour pulse tracer injection, into each well (well E1 and well C2), followed by a series of tracer-free water flushes. The flushing of the wells with tracer-free water continued until the second experiment, Experiment 2, began. Experiment 2 began on June 18, 2006 and lasted for three days. Experiment 2 consisted of a longer, eight-hour pulse tracer injection into Well C2 (Table 1). The three injections consisted of three phases: 1) pre-saturation, 2) tracer injection, and 3) tracer-free water flush. The pre-saturation phase consisted of a tracer-free water injection to wet up the flow path between the well and the stream, to minimize interference from the unsaturated zone. Immediately following the pre-saturation phase, the tracer injection began with the same Q_{inj} as the pre-saturation phase to access the same flow path

established during the pre-saturation phase. The flush phase immediately followed the tracer injection with the same Q_{inj} as the previous phases.

Table 1: Injection Summary

	Inj1	Inj2	Inj3
Well ID	E1	C2	C2
Upslope Distance from Trench (m)	15.2	8.9	8.9
Q_{inj} (L/hr)	3	2	18
Q_{trench} (L/hr)	76	206	46
Q_{inj} as % of Q_{trench}	4	1	39
Input Tracer Concentration (mg Br ⁻ /L)	123,000	123,000	113
Mass Injection rate (mg/hr)	369,000	246,000	2034
Length of Injection (hr)	1	1	8.2

3.2.1. Experiment One

Experiment 1 included two pulse tracer injections, Injection 1 (Inj1) and Injection 2 (Inj2), as well as a series of 27 flushes. Both Inj1 and Inj2 were short duration, high concentration pulse injections with low Q_{inj} (Table 1). The Q_{inj} 's for Experiment 1 were assumed to represent the average precipitation intensity of 3 mm/hr. The rates accounted for the size of the well and an assumed spreading of injected water 0.5 m on either side of the well. A tracer concentration of 123,000 mg Br⁻/L was used for both Inj1 and Inj2 to ensure an observable concentration.

3.2.1.1. Injection 1

Inj1 was performed on April 12, 2006 in well E1. During Inj1, the Q_{inj} was kept constant at 3 L/hr. Tracer-free water was injected for three hours to pre-saturate the flow path. Immediately following the pre-saturation, a tracer solution of 123,000mg Br⁻/L was injected at 3 L/hr for one hour (introducing a total of 369,000 mg Br⁻ into the subsurface). A 1.5 hrs tracer-free water flush immediately followed the tracer injection. Two days after Inj1, the movement of tracer was augmented by a rain storm, Storm1.

3.2.1.2. Injection 2

Well C2 was used for the second injection on April 19, 2006. Due to C2's shorter upslope distance from the trench a lower Q_{inj} (2 L/hr) was used. Tracer-free water was injected for 1.5 hrs to pre-saturate the flow path, followed by a tracer injection of 123,000mg Br^- /L, which introduced a total of 246,000 mg Br^- into the subsurface. A two hour tracer-free water flush immediately followed the tracer injection. Two days later well C2 received an additional tracer-free water flush, Flush1.

3.2.1.3. Flushes

After Storm1 and Flush1, it was deemed necessary to continue flushing the wells with tracer-free water. The objectives of the flushing were twofold: 1) to remove the bromide tracer from the flow path and 2) to observe the behavior of the tracer in the flow path under various conditions of antecedent wetness and injection rates. A total of 27 flushes were performed on both wells C2 and E1.

3.2.2. *Experiment Two*

On June 18, Experiment 2 began with a steady-state well injection, Inj3. The Q_{inj} (18 L/hr) for Experiment 2 was based on the observed build-up of water in the injection well, so as not to exceed the screened portion of the well. Tracer-free water was injected for five hours on the night of June 17 and 1.75 hours on the morning of the 18th to pre-saturate the flow path. A notable shift (~ 18.5 L/hr) in Q_{trench} that was approximately equal to Q_{inj} (~ 18 L/hr) signified the completion of the pre-saturation phase. Immediately following the pre-saturation phase, a tracer solution of 115 mg Br^- /L was injected for 8.2 hours (Table 1) until technical difficulties temporarily prevented further injection. The tracer concentration was selected to minimize the buoyancy-induced effects that could occur due to the

density difference between the tracer and the water already present in the system [Istok and Humphrey, 1995]. After 1.5 hours with no injection, an 8-hour tracer-free water flush began. The flushing was interrupted again for 2.75 hours, followed by an additional 24.5 hrs of flushing, with the exception of another 4.25 hr interruption. The interruptions were due to technical issues with the pumping system.

In Experiment 2, tracer was pushed out of the flowpath using an immediate and equal magnitude flush, rather than an injection followed by a long period of intermittent flush and drainage cycles. The flushing phase of Experiment 2 lasted for two days.

4. Results

4.1. Experiment One

4.1.1. Inj1 in well E1

Inj1 produced a BTC typical of a pulse tracer injection, with a short duration $[\text{Br}^-]_{\text{trench}}$ peak in relation to the long duration of the BTC (Figure 3). Some of the early concentration data are missing due to the ISE being calibrated with standard solutions during the beginning of the experiment. The $[\text{Br}^-]_{\text{trench}}$ from Inj1 peaked around 80 mg Br^-/L , after the injection ceased. During Inj1 and its initial BTC (i.e. the first rise and fall in measured concentration), Q_{trench} remained relatively constant. Inj1's contribution to Q_{trench} was minimal accounting for approximately 4% of Q_{trench} (Table 1). During the 48 hours immediately following Inj1, 13% of the injected tracer was recovered (Table 2). While a 5 mm rainstorm that occurred about 23 hours after Inj1 had little effect on the $[\text{Br}^-]_{\text{trench}}$, a larger 39.5 mm rainstorm, two days after Inj1 caused an increase in the $[\text{Br}^-]_{\text{trench}}$, suggesting that the storm mobilized some of the tracer remaining. After the first 25 mm of precipitation was added during the second rainstorm, Q_{trench} increased dramatically and diluted the $[\text{Br}^-]_{\text{trench}}$. While not shown, the mass flowrate increased with the increased Q_{trench} . The time to peak method yielded an average velocity of 4.45 m/hr (Table 3). Using the time to CoM method for the 48 hours immediately following Inj1, the average velocity was 1.1 m/hr (Table 3). CXTFIT was not used to calculate a velocity for Inj1.

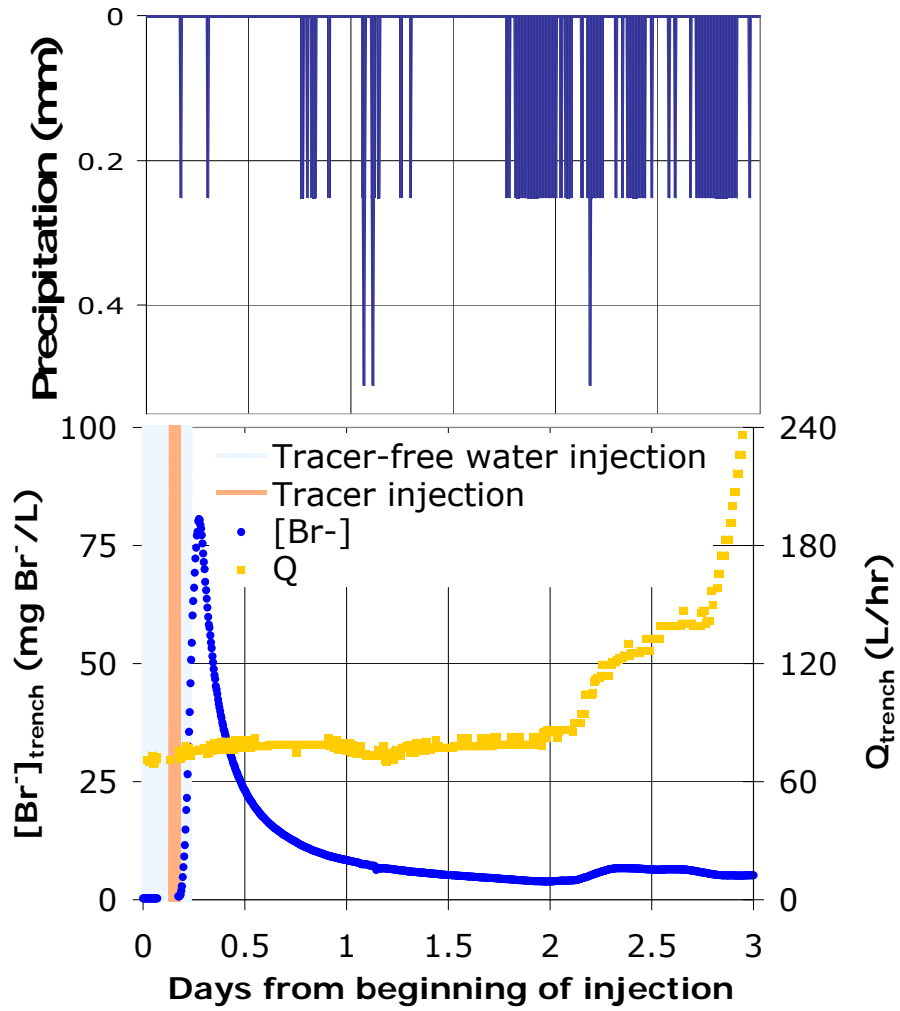


Figure 3: BTC for Inj1 with evidence of additional concentration rise due to precipitation 2 days post-injection

Table 2: Injection parameters and breakthrough curve results

	Inj1	Inj2	Inj3
Well ID	E1	C2	C2
Upslope Distance from Trench (m)	15.2	8.9	8.9
Q_{inj} (L/hr)	3	2	18
Q_{trench} (L/hr)	76	206	46
Q_{inj} as % of Q_{trench}	4	1	39
Input Tracer Concentration (mg Br ⁻ /L)	123,000	123,000	113
Mass Injection rate (mg/hr)	369,000	246,000	2034
% Recovery during injection	13	18	~90
Overall % mass recovered	64		>90
Center of Mass of Bromide (hrs)	10.5	14.5	8
Average velocity (m/hr) [Time to CoM]	1.45	0.63	1.13
Max. velocity (m/hr) [Mosley, 1982]	15.2	7	10.7
% Q_{inj} measured at trench	0	0	~100
Peak [Br ⁻] _{trench} (mg Br ⁻ /L)	80.6	23	27
Peak Q_{trench} (L/hr)	81.2	177	65.5
Peak Mass Flow (mg/hr)	11100	3325	1767
CoM input to Conc. Peak (min.)	175	230	260
Minutes from End of tracer to Conc. Peak	145	200	15
Minutes from End of Flush to Conc. Peak	60	75	N/A

Table 3: Summary of Velocities, Dispersion Coefficients and Dispersivities for Inj1, Inj2 and Inj3

	<i>Time to peak</i>	<i>Mosley</i>	<i>CXTFIT</i>		
	Velocity, v (m hr ⁻¹)		Velocity, v (m hr ⁻¹)	Dispersion coefficient, D (m ² hr ⁻¹)	Dispersivity, α (m)
Inj1 (E1)	4.45	1.12			
Inj2 (C2)	2.05	0.57			
E1 flushes		0.00029	0.020	1.6	83
C2 flushes		0.00015	0.006	0.76	127
Inj3 (overall)	1.08	0.62	0.78	1.7	2.2

[Br⁻]_{trench} measurements from the field ISE agreed with the measurements made using the laboratory IC (Figure 4 inset). However, the grab samples taken from the seep, at the upper end of the trench, diverged from the trench samples: increasing more rapidly and reaching much higher concentrations (Figure 4). This seep response indicated that E1's flowpath to the trench intersected the seep.

The $[\text{Br}^-]_{\text{trench}}$ is less than that at the seep due to dilution by water entering the trench through a pathway other than the seep.

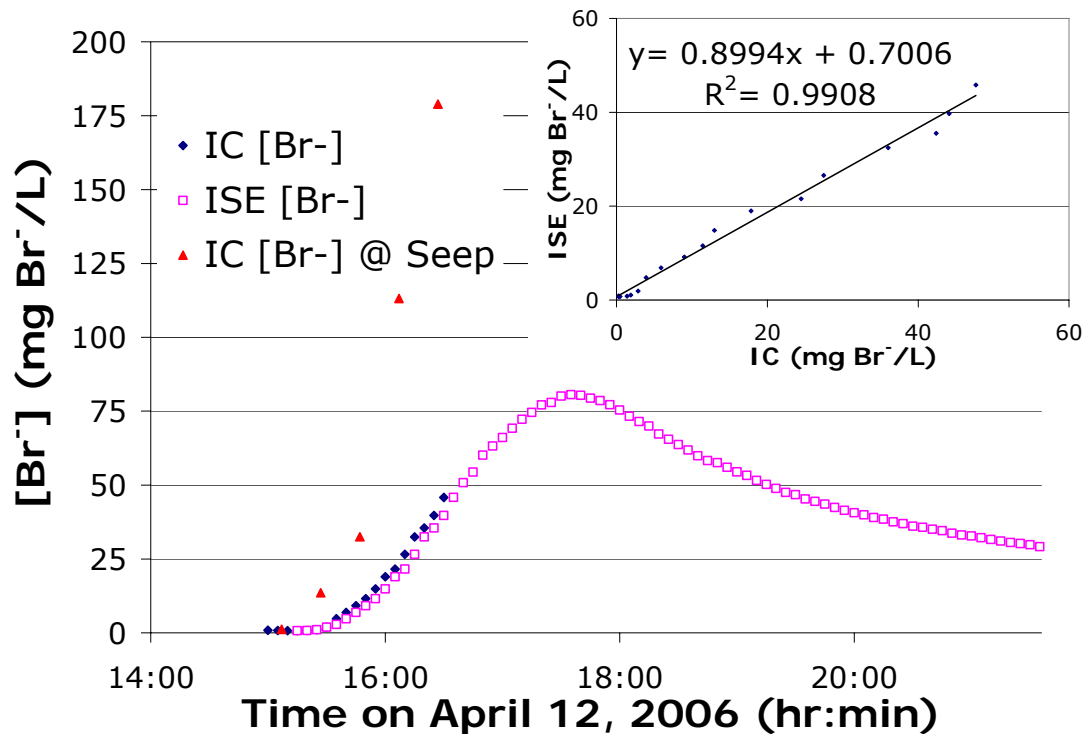


Figure 4: Inj1 calibration of in-situ field ISE (installed in the stilling basin) to the IC in the laboratory

4.1.2. Inj2 in well C2

Inj2's pulse tracer injection also produced a short-lived $[\text{Br}^-]_{\text{trench}}$ peak, post-injection (Figure 5). The $[\text{Br}^-]_{\text{trench}}$ from Inj2 peaked around 23 mg Br^-/L . Inj2's contribution to Q_{trench} was miniscule, accounting for approximately 1% of Q_{trench} . Q_{trench} decreased throughout Inj2 and its initial BTC. A small 1.25 mm precipitation event about 32 hours after Inj2 was not large enough to mobilize tracer remaining in either E1 or C2's flowpath. However, two days after Inj2 a tracer-free water flush into C2 mobilized some of the tracer causing a second

increase in the $[\text{Br}^-]_{\text{trench}}$, which peaked after the tracer-free water flush ceased. The time to peak method yielded an average velocity of 2.05 m/hr (Table 3). Using the time to CoM method for the 48 hours immediately following Inj2, the average velocity was 0.57 m/hr (Table 3). CXTFIT was not used to calculate a velocity for Inj2.

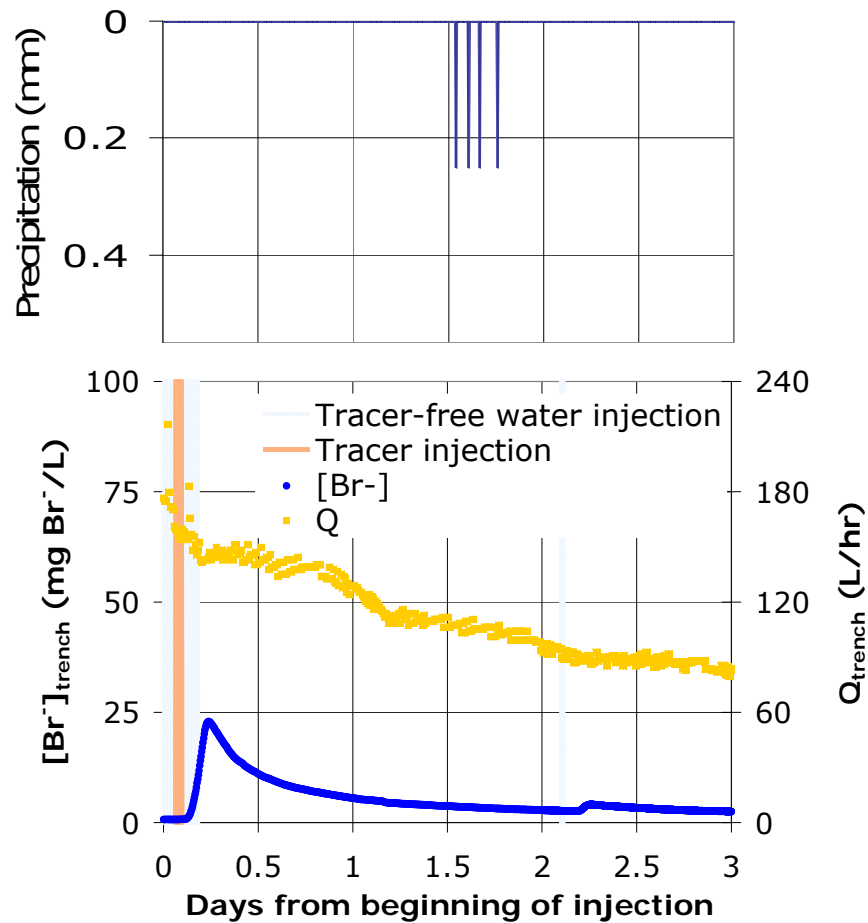


Figure 5: BTC Inj2 with evidence of additional concentration rise due to a tracer-free water flush 2 days post-injection

The field ISE measurements agreed with the IC measurements (Figure 6 inset). The grab samples taken from the seep at the upper end of the trench were measured using the laboratory IC and did not track the $[\text{Br}^-]_{\text{trench}}$ measurements. The $[\text{Br}^-]_{\text{seep}}$ did not increase during Inj2, Figure 6. Unlike E1 (Inj1), C2's flowpath did not appear to intersect the seep.

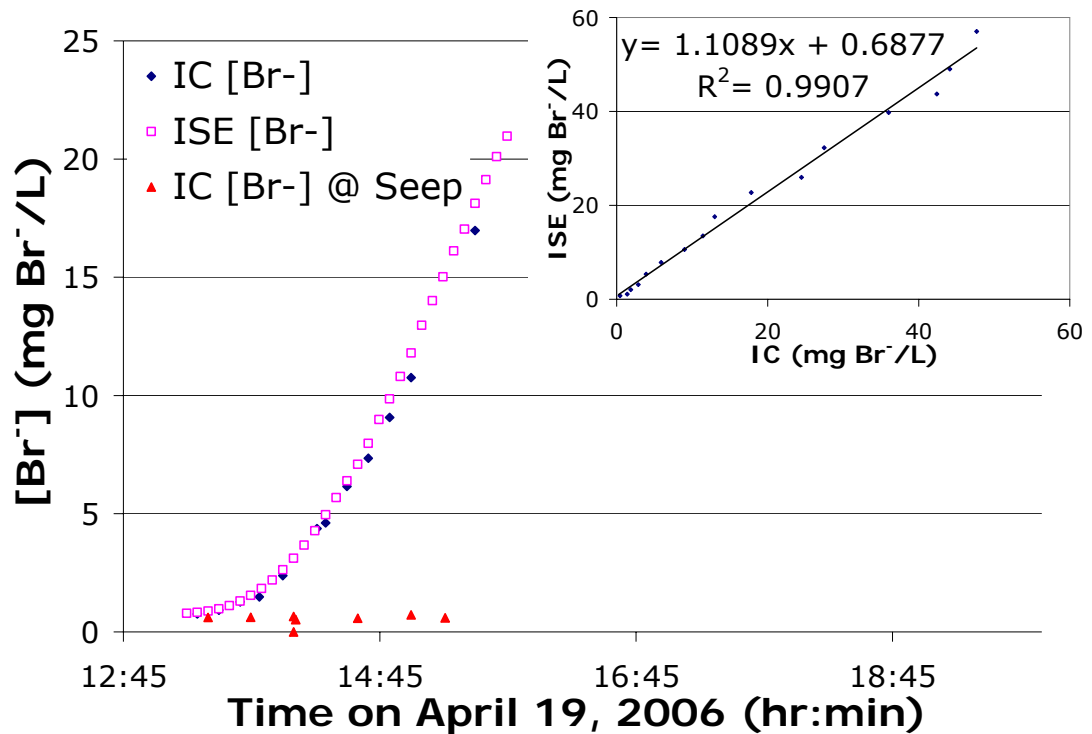


Figure 6: Inj2 calibration of in-situ field ISE (installed in the stilling basin) to the IC in the laboratory

4.1.3. Flushes

Figure 7 illustrates the percent of cumulative mass recovered during Experiment 1, from both wells with time from the beginning of Inj1, as well as the percent of cumulative water added to the system by both precipitation and flushing. The volume of water injected and volume equivalent precipitation (see Appendix B) were combined to couple the water added to the system into a single, cumulative

water parameter. Over sixty percent of the recovered mass was recovered within the first 400 hours, during which time only 20% of the cumulative water had been added.

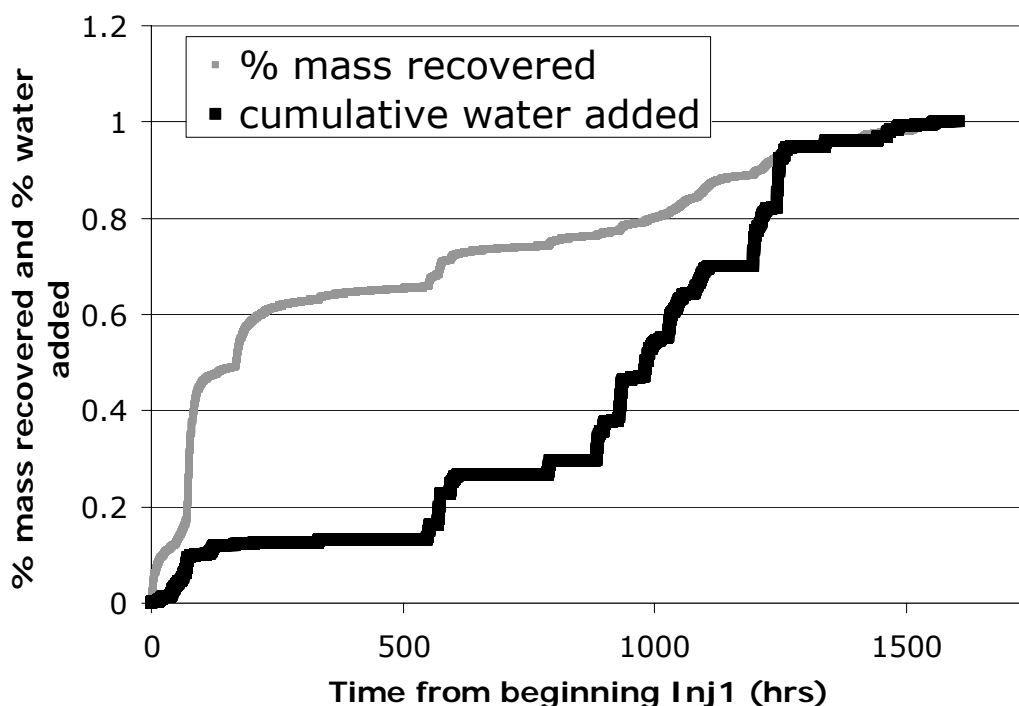


Figure 7: Cumulative mass recovered and cumulative water added (throughout the flushes) as a function of time from beginning of Inj1

Separate CXTFIT least-squares regressions were conducted for the E1 flushes and C2 flushes (Figures 8 and 9). CXTFIT calculated velocities of 0.02 and 0.006 m/hr, and dispersion coefficients of 1.6 and 0.76 m²/hr for E1 and C2, respectively (Table 3).

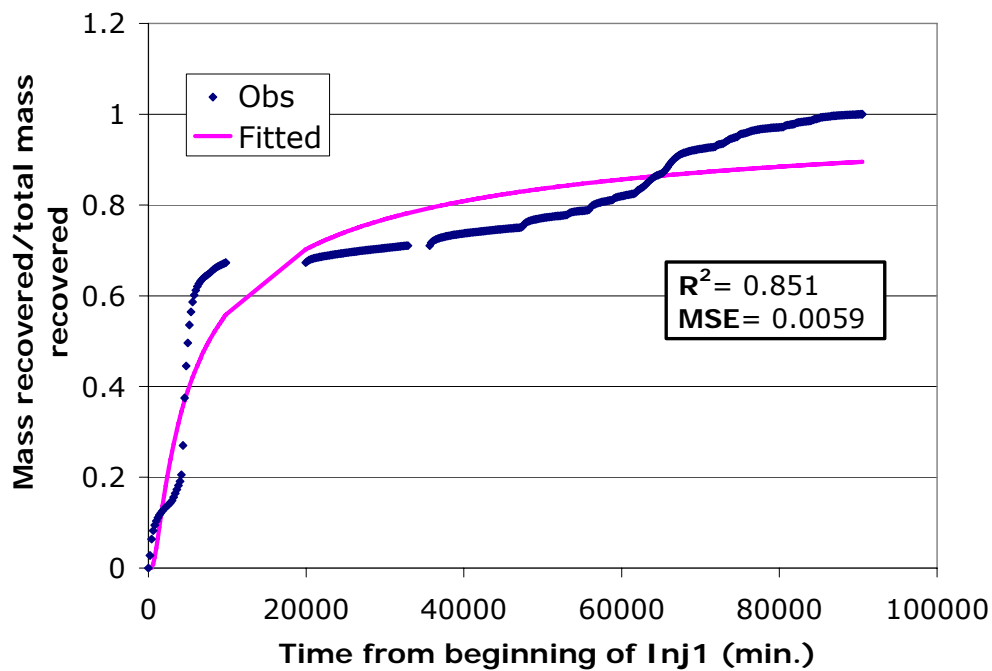


Figure 8: CXTFIT results for calculated velocity and dispersion coefficient for the E1 flushes

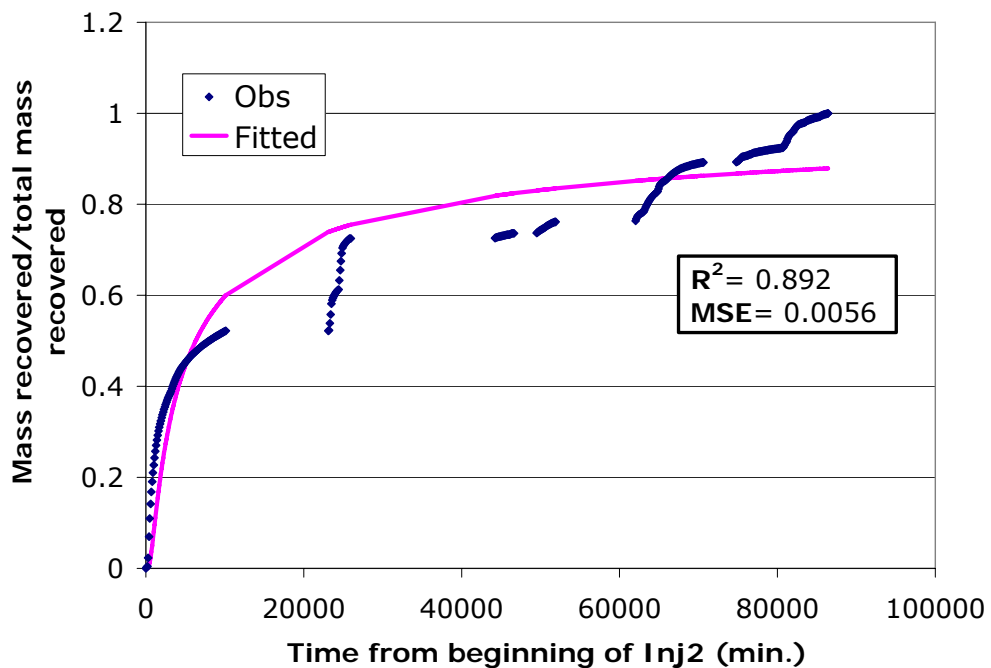


Figure 9: CXTFIT results for calculated velocity and dispersion coefficient for the C2 flushes

4.2. Experiment Two

Inj3's eight-hour pulse input of a low concentration tracer produced a peak of 27mg Br⁻/L, or 86% of the injected concentration, which coincided with the end of the tracer injection (Figure 10). Inj3's contribution to Q_{trench} accounted for approximately 39% of Q_{trench} (Table 2). The increases in Q_{trench} during the injecting/flushing and the decreases in Q_{trench} during the interruptions are evident (Figure 10). $[\text{Br}^-]_{\text{trench}}$ decreased rapidly with Q_{trench} during the injection interruptions (Figure 10). This drop is attributed to decreased flow entering the trench from the flowpath, (Figure 11, Appendix D). During Experiment 2, over 100% of the injected mass was recovered (Table 2) and the $[\text{Br}^-]_{\text{trench}}$ decreased to approximately 3 mg Br⁻/L, which was the $[\text{Br}^-]_{\text{trench}}$ at the beginning of the Inj3 tracer injection. The time to peak method yielded an average velocity of 1.08 m/hr (Table 3). Using the time to CoM method for the 48 hours immediately following Inj3, the average velocity was 0.62 m/hr (Table 3). Figure 12 shows the results of the CXTFIT least-squares regression based on Inj3's entire BTC. The CXTFIT average velocity and dispersion coefficient were 0.78 m/hr and 1.7 m²/hr, respectively (Table 3).

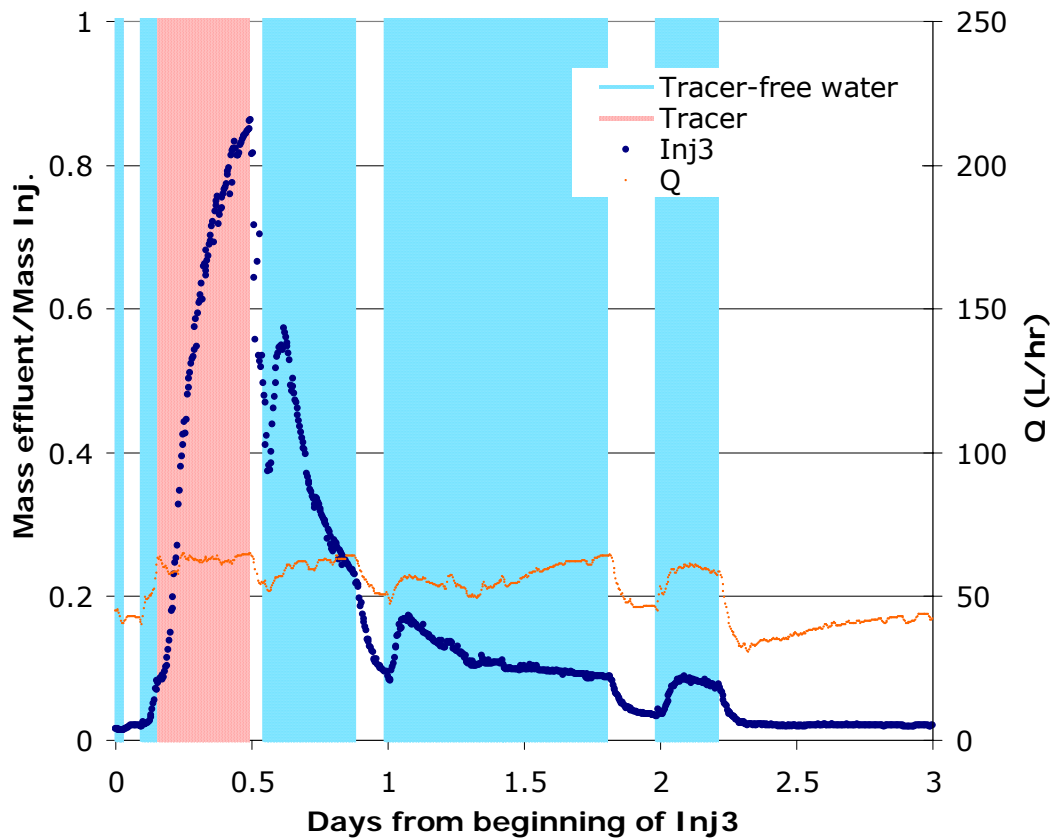


Figure 10: BTC for Inj3 showing injection and flush periods as well as the drops in volumetric flowrate and mass ratios during injection interruptions

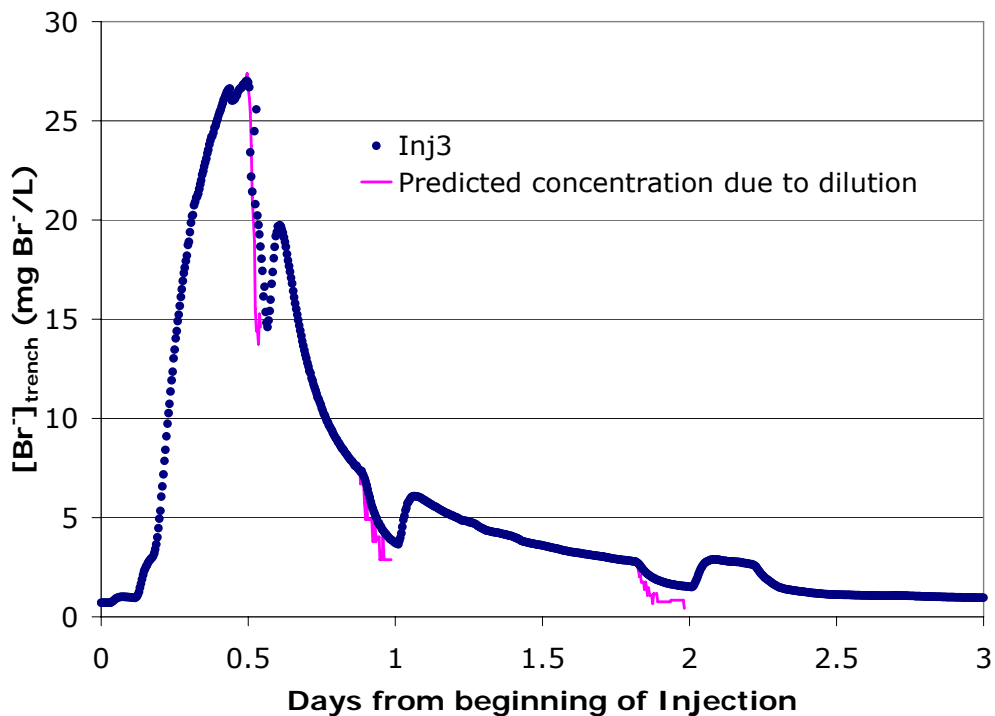


Figure 11: Theoretical drop in concentration due to decrease flowpath volumetric flowrate and dilution from seep flow

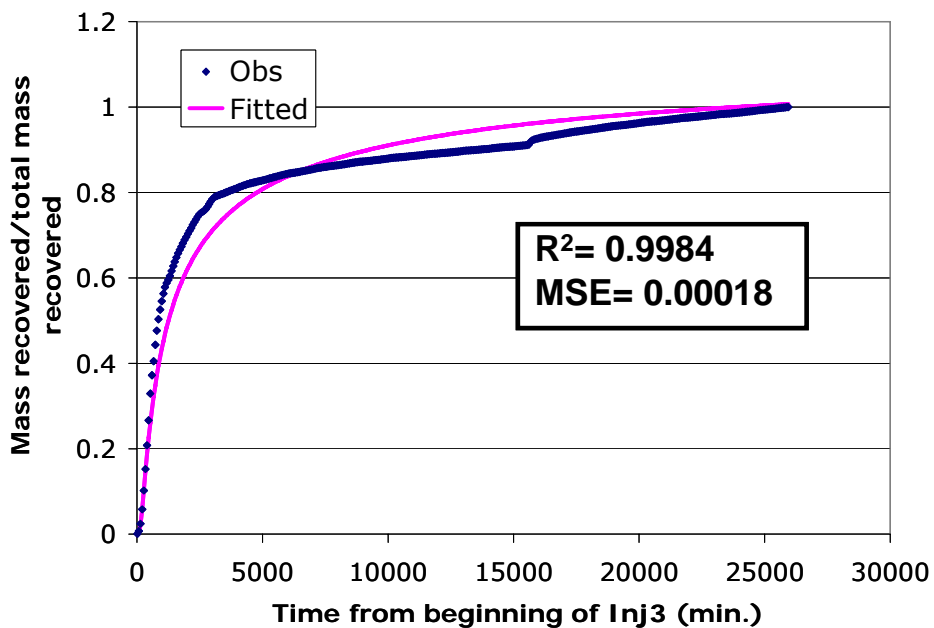


Figure 12: CXTFIT results for calculates of velocity and dispersion coefficient based on relative mass out of the trench during injection and flush phases of Inj3

5. Discussion: Characterization of lateral subsurface flow

To date, field-based hillslope hydrology studies have not quantified dispersion. While hillslope studies that have calculated velocities (i.e. the advective mechanism of transport) often observe evidence of dispersion, the accompanying discussions have tended to focus on other aspects of the observed responses (i.e. transit times and other directional transport issues [McGuire et al, 2007; Anderson et al, 1997; Tsuboyama et al, 1994]). As a result, we still do not know the effect of dispersion on the observed responses. However, due to the high velocities and additional preferential flowpaths, dispersion at the hillslope-scale should be larger than dispersion at the laboratory-scale and in groundwater systems.

Well injection tracer tests at the WS10 hillslope showed advection and dispersion rates larger than those reported from laboratory studies. Lateral preferential flowpaths appeared to significantly reduce travel time through the study hillslope. However, once tracer was stored in the subsurface, the travel times and average velocities depended largely on the hydraulic gradient (i.e. intensity and duration of precipitation and/or injection). The tracer tests also illustrated that as less tracer remained in the flowpath the amount of water required to remove the same quantity of tracer mass increased. These observed behaviors assist in the explanation of the calculated velocities and dispersivities and how they relate to fundamental hillslope hydrological processes.

5.1. Advection and dispersion quantified in two flowpaths at the hillslope-scale: Experiment 1

The quantification of advection and dispersion was complicated by a limited ability to control field conditions and by differences in flowpath characteristics. By using similar injection schemes in two wells, it was possible to compare different

methods for quantifying average velocities as well as investigate the dispersive component of transport. Time to peak calculations, based on Inj1 and Inj2 indicated that E1's velocity is nearly two times that of C2's. During a steady-state constant irrigation rate experiment [Anderson, 1997], where the peak was not caused by a decrease in the hydraulic gradient, the time to peak method accurately calculated the saturated subsurface flow velocities. The time to peak method was invalid for determining velocities for Inj1 and Inj2, since the times to peak during Inj1 and Inj2 were artifacts of a decreased hydraulic gradient. The decrease in the hydraulic gradient caused the peak to occur earlier than it would have under a constant hydraulic gradient, which resulted in larger apparent average velocities than actual.

The time to CoM method's reliance on the center of mass rather than the peak shifts the timing into the tail of the BTC. The time to CoM velocities are nearly one quarter of the time to peak velocities calculated from the initial BTC. The time to CoM velocities for Inj1 and Inj2 represent the average velocities for approximately 15% of the tracer, since the initial BTCs accounted for 15% of the total mass injected (12% from E1 and 16% from C2). 85% of the tracer that remained in the subsurface after Inj1 moved slower than the time to CoM velocities. Noting the low mass recovery, the time to CoM method was repeated to include the entire length of the flushes, Table 3. While 3-4 orders of magnitude lower than the time to CoM estimates from Inj1 and Inj2, the smaller velocities are an estimate for the long-term average velocity of the tracer recovered from the flowpaths. The velocities were highly variable during the series of flushes, with long draining cycles followed by brief injections. The long-term average velocity of the water through the flowpath includes periods of flow where

velocities were larger and smaller (near zero). The small long-term average velocities are indicative of long subsurface residence times. Both of the time to CoM calculations indicated that E1's velocity was nearly two times that of C2's, which agrees with the time to peak calculations as well as the observance of E1's connection to the seep. While both the time to peak and time to CoM methods quantify the advective portion of transport, neither account for the dispersive transport.

The CXTFIT average velocity for the E1 flushes was higher (~three times) than that for C2 flushes and two orders of magnitude larger than the time to CoM velocities for the E1 and C2 flushes, even with the same time intervals and the same mass recoveries. The time to CoM method is entirely dependent on the timing of the center of mass; however, tailing in the BTC caused by dispersion skews the timing to the right of the center of mass and decreases the calculated velocity. The dependence of the time to CoM method on a minimally disperse BTC, may make it a weak choice for accurately determining hillslope-scale advection. By simultaneously fitting both parameters to the observed transport and minimizing the error, CXTFIT may estimate the long-term average velocity and dispersion coefficient with more accuracy.

Figure 13 shows the BTCs of Inj1 and Inj2 with a normalized mass flowrate vs. time from beginning of tracer injection. By looking at the BTCs in relation to each other, it is difficult to conclude whether E1 or C2 exhibited more dispersion. However, the tailing on the BTCs indicates that dispersion occurred [Domenico and Schwartz, 2005; Schnoor, 1996]. Dispersion is difficult to discern from mere observation of the BTCs and requires a more intensive analysis. E1's dispersion coefficient calculated by CXTFIT is nearly twice that of C2's, indicating that the

solute spreads more in E1's flowpath than it does in C2's flowpath, which was not evident through visual inspection of the BTCs. Since ~90% of the mass was recovered from E1, the E1 dispersion results are probably more reliable than those from C2, where only 46% of the mass was recovered, even though the r^2 value from E1's fit ($r^2 = 0.851$) is smaller than C2's ($r^2 = 0.892$).

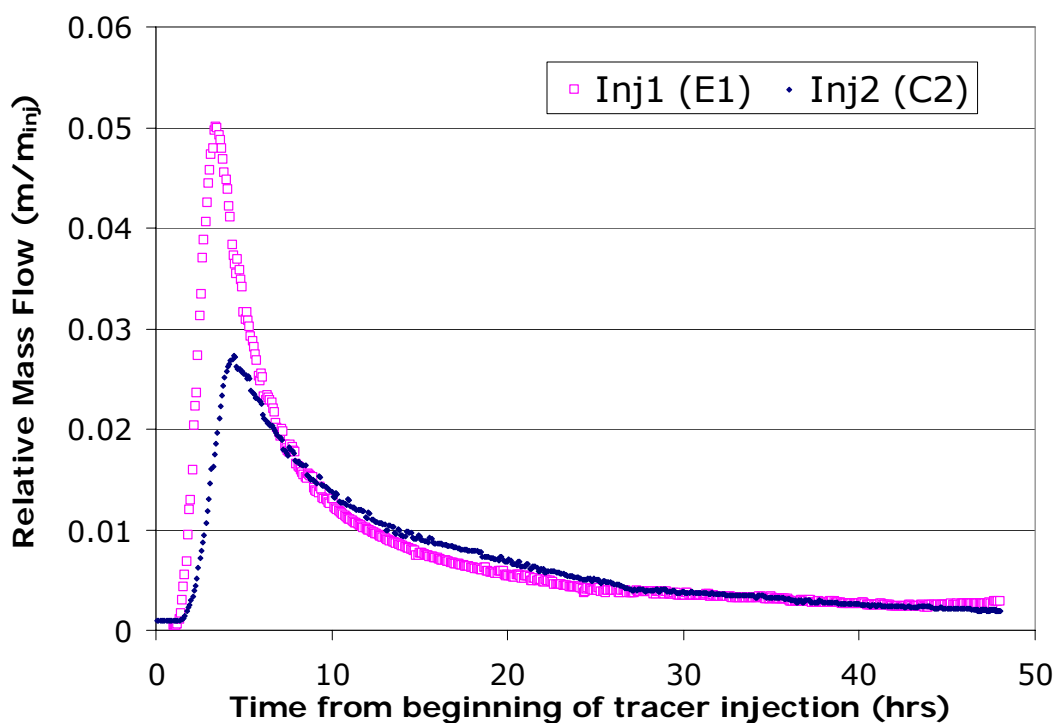


Figure 13: Initial BTCs Inj1 and Inj2

The dispersivity of E1's flowpath is smaller than that of C2's, meaning that for a given average velocity, E1 would have less spreading than C2. E1's flowpath is expected to have less spreading because the preferential flow path seen in E1 intersects the seep and delivers the tracer to the trench more efficiently. The water and tracer are able to travel in a more direct, less tortuous path, which results in less dispersion because there is less influence from the porous media.

While the flushes mimic what may be seen during a series of natural precipitation events, the cyclical pattern of flushing and draining during Experiment 1 created the appearance of dispersion due to the stored water rather than depicting the range of velocities. The water and tracer became stored in the soil due to either capillarity or the presence of a lens, probably not due to sorption, since bromide is a conservative tracer. This storage increased the transit time of the bulk of the tracer due to the intermittent release of tracer. The increase in transit time due to storage is a secondary mechanism (in addition to numerous and tortuous flowpaths) for causing dispersion [Schnoor, 1996].

5.2. Advection and dispersion quantified in one flowpath under different flow conditions: Experiment 2

Each of the three methods used for velocity calculations in this study have assumptions built in. The time to peak method relies on a high mass recovery coupled with a constant velocity (i.e. a constant hydraulic gradient) to ensure accurate estimates of velocity. The time to CoM method relies on a high mass recovery alone. CXTFIT has the most assumptions including high mass recovery; constant velocity (i.e. constant hydraulic gradient); one-dimensional transport; homogeneous soil; no retardation; and no sorption. While it is important to understand the assumptions implicit in calculations, it is difficult to satisfy all assumptions for a calculation. By conducting Experiment 2 on C2's flowpath it is possible to compare the responses observed from two injection scenarios and compare the results of the calculation methods when different assumptions are not satisfied (Table 4). Velocities, dispersion coefficients and dispersivities for Inj3 are shown in Table 3.

Table 4: Assumptions by method (X indicates assumption satisfied)

Method	Assumption	Inj1	Inj2	Inj3
<i>Time to Peak</i>	High mass recovery			X
	Constant velocity			X
<i>Time to CoM</i>	High mass recovery			X
<i>CXTFIT</i>	High mass recovery			X
	Constant velocity			X
	One-dimensional flow	X		X
	Homogeneous			
	No retardation	X	X	X
	No sorption	X	X	X

The time to peak velocity calculated for Inj3 was 50% of that calculated for the same flowpath during Inj2. The discrepancy in calculated velocities and their divergence from the other velocities calculated, illustrates the effect of using the time to peak method for calculating velocities when the assumptions implicit in the theory are not satisfied (Table 4). Since Inj3 had a near constant hydraulic gradient, it was expected to have reached its peak earlier and have a higher velocity. However, since Inj2's peak was artificially induced the time to peak method resulted in an erroneously calculated velocity.

While the time to peak velocities of Inj2 and Inj3 differ by a factor of two, the time to CoM velocities for Inj2 and Inj3 were nearly the same. This similarity suggests that the time to CoM method may be valid for individual BTCs and short-term velocity calculations, regardless of the mass recovery (Table 4). As seen in the velocities calculated from the flushes, the long-term average velocity of transport through a flowpath is considerably smaller than the short-term velocity due to the fluctuations in the hydraulic gradient. Inj3's calculated time to peak

velocity was closer to its time to CoM velocity than Inj2's because Inj3 was closer to the ideal scenario (Table 4) for using the time to peak method.

The CXTFIT average velocity was in between Inj3's time to peak and time to CoM velocities, though all three were relatively close with the smallest velocity equal to over 60% of the largest. The CXTFIT average velocity is two orders of magnitude larger for Inj3 than it is for the C2 flushes. CXTFIT's constant velocity assumption while grossly violated during Inj2, was a valid assumption during Inj3 (Table 4). The Inj3 dispersion coefficient is over two times larger than the C2 flush dispersion coefficient (Table 3). Since the dispersion coefficient is directly related to the velocity [Schnoor, 1996], the dispersion coefficient from Inj3 being larger than from the C2 flushes is expected.

The dispersivity for Inj3 is two orders of magnitude smaller than that for the C2 flushes. This disparity in dispersivities is partially due to the difference in saturation level of the flowpath. Maraqa et al, [1997; Hutchison et al, 2003] found that a dispersivity calculated from measurements in unsaturated soils is higher than that calculated from measurements in a saturated or nearly saturated soil. Since storage during draining periods (i.e. those with a decreasing or non-existent hydraulic gradient) increases the apparent dispersion, the dispersion coefficient calculated from the flushes is likely overestimated. In addition, the advective movement of the tracer downslope occurs mainly during flushing, when a hydraulic gradient is present. However, CXTFIT assumes a constant velocity, which averages the short periods, when there is a higher lateral velocity, and long periods, when there is a minimal lateral velocity probably underestimating the effective advective movement. The likely overestimate of the dispersion

coefficient coupled with the likely underestimate of velocity, likely results in an overestimate of dispersivity.

5.3. *Comparison of velocities and dispersivities with other studies*

Previous calculations of subsurface lateral Darcy velocity for the top 110 cm of soil in WS10 ranged between 0.0005 and 0.0045 m/hr [Harr, 1977] (Table 5)

Assuming a porosity of 0.65 [Ranken, 1974], Harr's [1977] Darcy velocities convert to average velocities of 0.0008 and 0.007 m/hr (Table 5). While the CXTFIT average velocity calculated from the C2 flushes falls within the range of Harr's calculated lateral subsurface velocities, the CXTFIT average velocity calculation from Inj3 far exceeds the range (Table 5). This may indicate that Harr's [1977] observations were mainly of unsaturated flow. Measurements made at saturation rarely mimic behavior that occur under natural conditions however, they are invaluable since they allow for determination of parameters under a controlled condition. Inj3 rendered the smallest range of calculated velocities due to control imposed by long-term saturated conditions with constant Q_{inj} . Therefore, it is likely that CXTFIT calculations based on Inj3 are the most accurate.

Table 5: Velocities calculated from Experiments 1 and 2, Harr and McGuire for WS10 hillslope

Velocity (m/hr)	E1 flushes	C2 flushes	Inj3	Harr
Darcy				0.0005 - 0.0045
Average	0.02	0.006	0.78	0.0008 - 0.007*

* - indicates value calculated based on a porosity of 0.65

Velocity (m/hr)	Inj1	Inj2	Inj3	McGuire
Time to Peak	4.45	2.05	1.08	0.47 - 0.82

Inj3's average velocity may provide insight into where within the soil/subsoil profile the flow is occurring. Dynamic cone penetrometer data [Van Verseveld, unpublished] shows that resistance increases at 40 cm in the location of C2 [Appendix G], which indicates shallower subsoil than in other areas of WS10. Since Inj3 occurred near the abrupt vertical change in resistance (assuming that the resistance change corresponds to an abrupt change in hydraulic conductivity), it is feasible that the dominant flowpath may include the subsoil. If we assume the subsoil K_s is 0.20-0.50 m/hr [Harr, 1977], this results in lateral Darcy velocities of 0.10 to 0.25 m/hr, based on a gradient of 0.5 [Harr, 1977], which correlates to average velocities of 0.15 to 0.38 m/hr based on a porosity of 0.65 [Ranken, 1974]. The subsurface average velocity range is within 20-50% of the CXTFIT calculated saturated average velocity of 0.78 m/hr, which may indicate that transport during Inj3 occurred in the subsoil. From the analysis of soil cores, Ranken [1974] stated that the subsoil has the greatest probability for saturated lateral movement, due to its small pores and high moisture content. Therefore, the use of a steady-state tracer injection appears to be a reasonable test for estimating saturated flowpath velocities, when used with a least-squares fit to the 1-D ADE.

McGuire et al [2007] conducted two line source tracer tests on the same slope in WS10, using precipitation to create the hydraulic gradient. AGA and Br^- tracers applied at 19 and 33 m upslope from the trench, respectively, resulted in observed subsurface flow time to peak velocities of 0.47 and 0.82 m/hr [McGuire et al, 2007] (Table 5). While comparable to the CXTFIT and time to peak Inj3 velocities, this range is much less than the CXTFIT and time to peak flush velocities. As the McGuire et al [2007] line source tests occurred during the wet

season, the results may be indicative of saturated flow velocities as they were comparable to the velocity calculation from Inj3. The subsurface flow velocities calculated may be good for comparison with each other and give a reasonable estimate for a short-term velocity, however; the application of the method is flawed. Using the difference in time between precipitation initiation and peak mass flow to calculate a velocity is feasible under certain conditions, such as a known saturated condition with a constant hydraulic gradient throughout the rise to peak, as in Anderson et al [1997]. However, without controlled conditions it is not a valid method. As seen in both Inj1 and Inj2 the peak time was dictated by a decrease in the hydraulic gradient (i.e. flushing or injection), not because it took that long for the majority of the tracer injected to reach the outlet. The artificially induced peak in Inj1 and Inj2 is similar to what may occur after precipitation stops (i.e. when the hydraulic gradient decreases), as was the case for McGuire et al [2007]. The early peak resulted in calculated time to peak velocities much larger than the time to CoM and CXTFIT calculations.

Empirical values of field-scale longitudinal dispersivity for unconsolidated porous media are shown in Table 6 [Schnoor, 1996]. All of the dispersivities calculated using CXTFIT (Table 7) for both flowpaths fall within the orders of magnitude reported for the applicable field-scales (Table 6). Since the length of the WS10 hillslope is much longer than the length of the flowpaths examined, it is likely that the dispersivity of the hillslope is larger than calculated, as dispersivity tends to increase with scale and transport distance [Domenico & Schwartz, 1998; Schnoor, 1996; Gelhar, 1992]. As two of the dispersivities calculated from these three experiments are rather large (at the high end of the reported range of empirical

values), it appears that dispersion, either apparent or real, indeed plays an important role in solute transport at the hillslope-scale.

Table 6: Empirical Values for unconsolidated porous media [Schnoor, 1996]

Description	Scale, m	Longitudinal Dispersivity, α , m	
		Average	Range
Laboratory	<1	0.001-0.01	0.0001-0.01
Field, Small-scale	1-10	0.1-1.0	0.001-1.0
Field, Large-scale	10-100	25	1-100

Table 7: CXTFIT calculated values from Experiments 1 and 2

	Scale, m	Longitudinal Dispersivity, α , m
E1 Flushes	15.2	83
C2 Flushes	8.9	127
Inj3	8.9	2.2

5.4. Why quantify velocities and dispersivities?

Assessment of the importance of fundamental mass transfer mechanisms at the hillslope-scale not only solidify fundamental knowledge regarding the importance of hillslope-scale hydraulic processes, but also provide insight into what may be overlooked in models. This report attempts to illuminate the interdependence of velocity and dispersion and the importance of quantifying rather than qualifying dispersion.

Since tracers are used to describe water movement through hillslopes, it is important to understand the fundamental transport mechanisms that affect the movement of solutes with water [Schnoor, 1996]. Quantifying solute movement accurately at the hillslope-scale is important for predictions of land use effects on

water quality. As velocities and dispersivities are directly intertwined, it is important to determine both parameters.

Dispersive effects on observed solute concentrations may lead to better estimates of where subsurface stormflow originates [Jones et al, 2006] and illuminate the validity of mixing assumptions. The measurement of tracer as it moves through the subsurface provides valuable information of the spatial variability of a flowpath. While quantification of the advective velocity describes the movement of the center of mass through the subsurface, quantification of the dispersion illuminates the distribution of mass about the advective front.

By calculating advection and dispersion, it was possible to determine how much spreading and mixing/dilution occurred. As seen in the calculation of velocities and dispersion coefficients for Inj1, Inj2 and Inj3 we were able to not only learn how fast the advective front (CoM) moved downslope, but also how dispersion occurred during that movement. Through the quantification of advection and dispersion in Experiment 1, it was shown not only that one flowpath had a larger advective velocity but also mixed with the tracer-free water more due to its higher velocity. In addition, the dispersion coefficients showed that while Inj1 and Inj2 have very similar BTCs, Inj2's dispersion coefficient was about twice that of Inj1's, indicating that Inj2 spread longitudinally more than Inj1. Through the quantification of advection and dispersion in Experiment 2, the large effect of stored water on apparent dispersion was illustrated. As stored water plays a leading role in the hillslope hydrology, accounting for the dispersion that results from storage it is imperative to accurately describing internal hillslope hydrological processes.

6. Conclusions

This study used a well-injection technique originally developed for groundwater investigations to interrogate internal lateral subsurface flow processes on a forested hillslope. Tracer injections into two wells have shown evidence of preferential flow in at least one of the wells, small long-term average velocities coupled with large short-term average velocities, and the effects of tracer storage on BTCs. Analysis of the tracer data recovered from these experiments showed that care must be taken when using a method to calculate a velocity from a BTC. In addition, the time to CoM method appeared to describe short-term average velocities well, but underestimated long-term average velocities due to the storage of water in the subsurface. CXTFIT proved to be an adequate tool for determining average velocities and dispersion coefficients, especially when the experiment satisfied the constant velocity assumption. Dispersion was prominent in the transport of water through the study hillslope and should be investigated more thoroughly on this and other study hillslopes.

BIBLIOGRAPHY

- Anderson, S.P., Dietrich, W.E., Montgomery, R.T., Conrad, M.E., & Loague, K. (1997) Subsurface flow paths in a steep, unchanneled catchment. *Water Resources Research*, 33(12), 2637-2653.
- Bedient, P.B., Rifai, H.S., & Newell. C.J. (1997) *Ground Water Contamination: Transport and Remediation*. New Jersey: Prentice Hall. p. 163.
- Beven, K. (2006). *Streamflow generation processes*. Benchmark papers in hydrology, no. 1. Wallingford: International Association of Hydrological Sciences.
- Brooks, E.S., Boll J., & McDaniel, P.A. (2004) A hillslope-scale experiment to measure lateral saturated hydraulic conductivity, *Water Resources Research*, 40, W04208
- Brusseau, M.L. (1993) The influence of Solute Size, Pore Water Velocity, and Intraparticle Porosity on Solute Dispersion and Transport in Soil. *Water Resources Research*, 29(4), 1071-1080.
- Domenico, P.A., & Schwartz, F.W. (1998) *Physical and Chemical Hydrogeology*. New York: John Wiley and Sons, Inc. pp. 215-236.
- Gelhar, L.W., Welty, C. & Rehfeldt, K.R. (1992). A Critical Review on Field-Scale Dispersion in Aquifers. *Water Resources Research* 28(7), 1955-1974.
- Harr, R. D. (1977) Water flux in soil and subsoil on a steep forested slope. *Journal of Hydrology*, 33, 37-58.
- Hewlett, J. D. & Hibbert, A. R. (1963) Moisture and Energy Conditions within a Sloping Soil Mass during Drainage. *Journal of Geophysical Research*. 63(4). 1081-1087.
- Hutchison, J.M., Seaman, J.C., Aburime, S.A., & Radcliffe, D.E. (2003). Chromate Transport and Retention in Variably Saturated Soil Columns. *Vadose Zone Journal*, 2, 702-714.
- Istok, J.D., & Humphrey, M.D. (1995) Laboratory Investigation of Buoyancy-Induced Flow (Plume Sinking) During Two-Well Tracer Tests. *Ground Water*. 33(4), 597-604.
- Jones, J.A. (2000) Hydrologic processes and peak discharge response to forest removal, regrowth, and roads in 10 small experimental basins, western Cascades, Oregon. *Water Resources Research*, 36(9), pp. 2621-2642.
- Jones, J.P., Sudicky, E.A., Brookfield, A.E., & Park, Y.-J. (2006) An assessment of the tracer-based approach to quantifying groundwater contributions to streamflow. *Water Resources Research*, 42, W02407.

Maraqqa, M.A., Wallace, R.B., & Voice, T.C. (1997) Effects of degree of water saturation on dispersivity and immobile water in sandy soil columns. *Journal of Contaminant Hydrology*, 25, 199–218.

McGuire, K.J., J.J. McDonnell, & Weiler, M. (2007) Integrating tracer experiments with modeling to assess runoff processes and water transit times. *Advances in Water Resources*, 30, 824-837.

Mosley, M.P. (1982) Subsurface Flow Velocities Through Selected Forest Soils, South Island, New Zealand. *Journal of Hydrology*, 55, 65-92.

Nyberg, L., Rodhe, A., Bishop, K. (1999) Water transit times and flow paths from two line injections of ^3H and ^{36}Cl in a microcatchment at Gårdsjön, Sweden. *Hydrological Processes*. 13, 1557-1575.

Ranken, D.W. (1974) Hydrological properties of soil and subsoil on a steep, forested slope. M.S. Thesis, Oregon State University, Corvallis.

Rodhe, A., Nyberg, L., & Bishop, K. (1996) Transit times for water in a small till catchment from a step shift in the oxygen 18 content of the water input. *Water Resources Research*, 30(12), 3497-3511.

Rothacher, J., Dyrness, C.T., & Fredriksen, R.L. (1967) Hydrologic and related characteristics of three small watershed in the Oregon Cascades, U.S. Department of Agriculture, Forest Service, Pacific Northwest Forest and Range Experiment Station, Portland, OR.

Schnoor, J.L. (1996) Environmental Modeling: Fate and Transport of Pollutants in Water, Air and Soil. New York: John Wiley and Sons, Inc., pp. 471-473.

Sidle, R.C. (2006) Field observations and process understanding in hydrology: essential components in scaling. *Hydrological Processes*, 20, 1439-1445.

Swanson, F.J. & James, M.E. (1975) Geology and geomorphology of the H.J. Andrews Experimental Forest, western Cascades, Oregon., Res. Pap. PNW-188, U.S. Department of Agriculture, Forest Service, Pacific Northwest Forest and Range Experiment Station, Portland, OR.

Toride, N., F.J. Leij, and M. Th. van Genuchten,(1999) The CXTFIT Code for Estimating Transport Parameters from Laboratory or Field Tracer Experiments,, Version 2.1, Research Report No. 137, U.S. Salinity Laboratory, USDA, ARS, Riverside, CA.

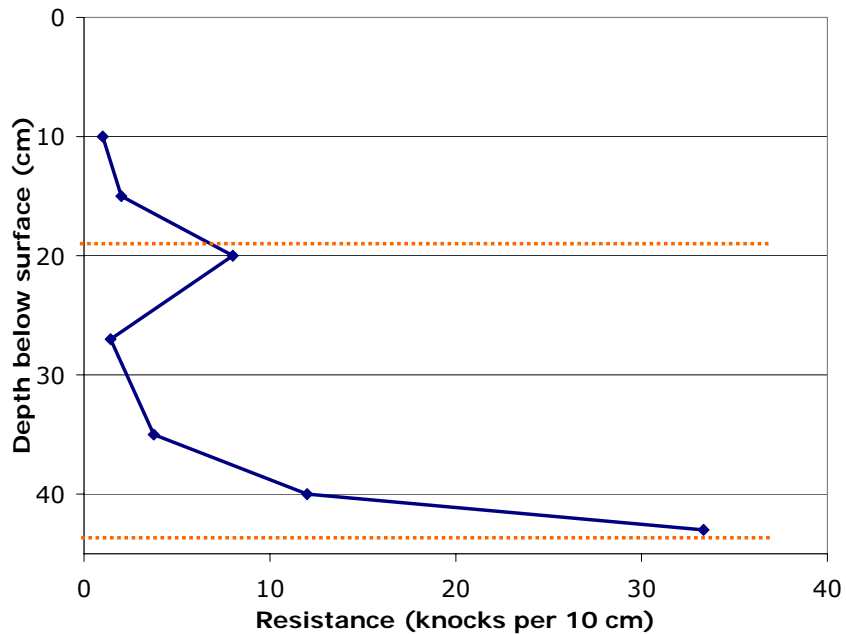
Tsuboyama, Y. Sidle, R.C., Noguchi, S., & Hosoda, I. (1994) Flow and solute transport through the soil matrix and macropores of a hillslope segment. *Water Resources Research*, 30(4), 879-890.

Vanderborght, J., Timmerman, A., & Feyen, J. (2000) Solute transport for steady-state and transient flow in soils with and without macropores. *Soil Science Society of America Journal*, 64, 1305-1317.

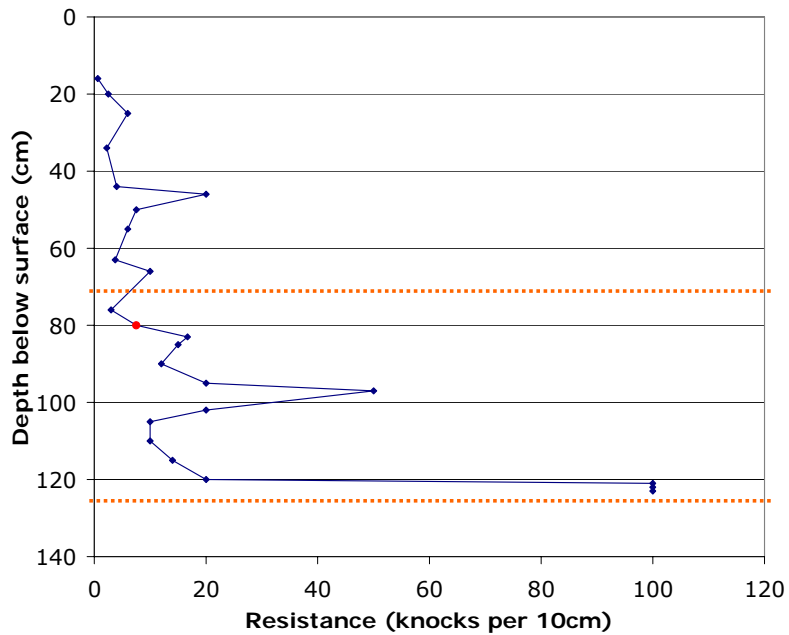
Vanderborght, J., Gähwiler, P., & Flühler, H. (2002) Identification of transport processes in soil cores using fluorescent tracers. *Soil Science Society of America Journal*, 66, 774-787.

APPENDICES

Appendix A: Dynamic Cone Penetrometer Profile



Appendix Figure 1: Dynamic Cone Penetrometer profile at well C2



Appendix Figure 2: Dynamic Cone Penetrometer profile at well E1

Appendix B: Volume Equivalent Precipitation calculation

The Volume equivalent precipitation was calculated from an estimated surface area of the E1 and C2 flowpaths. The area was calculated using the distance upslope as the length and 0.3m as the width for both.

Ground surface area of flowpaths= $15.2\text{m} \times 0.3\text{m} + 8.9\text{m} \times 0.3\text{m} = 7.23 \text{ m}^2$

Precipitation values were converted from mm to m and then multiplied by the ground surface area to get a volume equivalent.

The volume equivalent precipitation in m^3 was then converted to L by multiplying by $(1000 \text{ L}/\text{m}^3)$

Appendix C: Determination of Mass recovered per well

If mass recovered was a result of the initial injection flow or the result of flushing a specific well, the entire mass

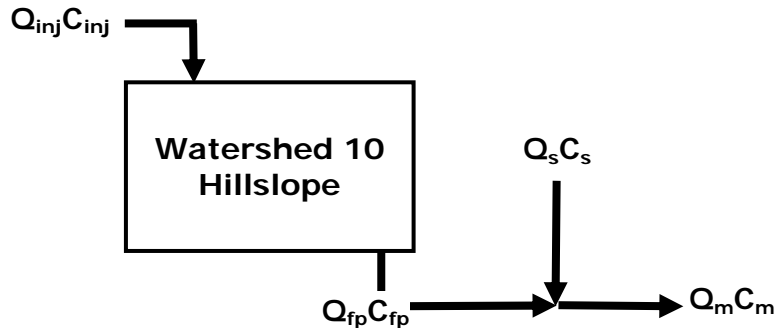
Mass recovered was attributed to a specific well if due to a single well flush.

Mass recovered due to a precipitation event or flushing in both wells simultaneously was divided evenly between both C2 and E1.

In one case 10% of the mass recovered was attributed to C2 while the other 90% was attributed to E1. In this case, there was a large precipitation event while flushing E1 amounting to ~24L of water added to each the flowpaths which was 10% of the total flush volume.

The precipitation event influenced the mass flow and based on estimated surface area of C2's pathway corresponded to a volumetric flowrate of approx. 37L/hr. The injection into E1 was 33.3 L/hr. Since half of the precipitation contributed to the flushing of C2 and half E1, an estimated 18.5 additional L/hr of water flushed E1 while only 18.5L/hr flushed C2. Resulting in 51.8 L/hr flushing E1 and about 25% of the flushing flow going to C2.

Appendix D: Theoretical concentration drop due to flowpath drop



Appendix Figure 3: Flowchart of hillslope system with well injection

$Q_{inj}=0$ when pump stops
 When $Q_{inj}=0$, $Q_{fp} = 0$ as the flowpath drains

$$Q_{fp} \approx Q_m - Q_s$$

During Injection period, at steady-state $Q_{fp}=Q_{inj} \approx 18\text{L/hr}$

When injection stops, $Q_{fp}=Q_m-Q_s$, where $Q_s=Q_m-18\text{L/hr}$ just before $Q_{inj}=0$

Hypothesis:

As Q_{fp} decreases C_m decreases due to dilution from Q_{seep}

During a break in injection:

$$C_{fp}=110 \text{ mg Br-/L}$$

$$C_s=0.71 \text{ mg Br-/L}$$

$$C_{mest} = \frac{Q_s \times C_s + (Q_m - Q_s) \times C_{fp}}{Q_m} = \frac{Q_s \times 0.71 + (Q_m - Q_s) \times 110}{Q_m}$$

The C_{mest} equation estimated the concentration change expected due to the decreased volumetric flowrate from the flowpath while the volumetric flowrate from the seep remained essentially constant.